Cyclic four-spin exchange on a two-dimensional square lattice: Possible applications in high-T_c superconductors

M. Roger
Département de Physique Générale, Service de Physique du Solide et de Résonance Magnétique, Commissariat à l'Energie Atomique, Centre d'Etudes Nucléaires de Saclay, 91191 Gif-sur-Yvette, Cedex, France

J. M. Delrieu
29 rue de la Feverie, 91190 Gif-sur-Yvette, France
(Received 8 August 1988)

In the planar CuO_2 square lattice of new superconductors, the small energy difference of conducting holes between Cu and O sites, compared to the relatively large on-site energy for double occupancy, might favor cyclic four-hole exchange via intermediate O sites rather than superexchange processes, as in solid ^{3}He. The properties of the four-spin exchange and Heisenberg Hamiltonians are compared in two dimensions through exact diagonalization on small clusters up to 18 spins. Four-spin exchange could explain the large inelasticity observed in neutron and two-magnon Raman spectroscopy, and resolve some discrepancies between exchange frequencies deduced from Raman and susceptibility data.

The presence of two-dimensional (2D) conducting CuO_2 planes with a square lattice of copper atoms connected through oxygen is essential for the physics of copper-based high-T_c superconductors.[1] The most common current picture is a Hubbard Hamiltonian on the Cu sites with transfer energy $t_{\text{Cu-Cu}}$ and on-site repulsion U_{Cu}. However, for some transition-metal oxides, the energy difference $\varepsilon = \varepsilon_p - \varepsilon_d$ for a hole occupying a metal or an oxygen site is small compared to the energy U for double-hole occupancy.[2] It is particularly weak in copper oxides ($\varepsilon \sim 0.4$ eV compared to $U \sim 8$–10 eV from experiments[1]) and the role played by intermediate O sites must be taken more precisely into account. The more realistic extended Hubbard Hamiltonian proposed in Ref. 2 has been recently applied to new superconductors:[3]

$$\mathcal{H} = \sum_{i,\sigma} \varepsilon_\alpha n_{i\sigma} + t \sum_{i,j,\sigma} c_{i\sigma}^\dagger c_{j\sigma} + V \sum_{i<j} \sum_{\sigma,\sigma'} n_{i\sigma} n_{j\sigma'} + \sum_i U_\alpha n_{i\downarrow} n_{i\uparrow} , \quad (1)$$

where $c_{i\sigma}^\dagger$, $c_{i\sigma}$, and $n_{i\sigma}$ represent, respectively, the creation, annihilation, and number operators for holes on Cu or O sites. The ε_α are on-site energies for single-hole occupancy, depending on the O($\alpha = p$) or Cu($\alpha = d$) site. t is the hopping frequency. The U_α are on-site energies for double occupancy of holes. V is the Coulomb repulsion between first-neighbor holes.

This Hamiltonian includes fundamental correlations involving intermediate O sites that are neglected in the simple Hubbard model. In particular, in the large-U limit, exchange processes between holes should be very similar to those occurring in hard-core quantum fluids.[4–6] The large-U energies prevent two holes from crossing on the same site as shown in Fig. 1(a); but four holes can exchange cyclically through eight successive hops via intermediate O sites [Fig. 1(b)], involving lower potential barriers ($V \sim 1$ to 2 eV, $\varepsilon \sim 0.4$ eV).

The possibility of "ring exchange" between fermions was put forward some time ago[4] and was substantiated recently in solid ^{3}He. Cyclic four- and three-particle exchanges account for all unusual magnetic properties of the bcc solid.[6] Delrieu, Roger, and Hetherington[5] have also predicted, from simple steric arguments, dominant three-spin exchange in compact triangular geometries (3D hcp ^{3}He or 2D triangular lattice), leading to ferromagnetism. This has been confirmed experimentally in the hcp solid[7]

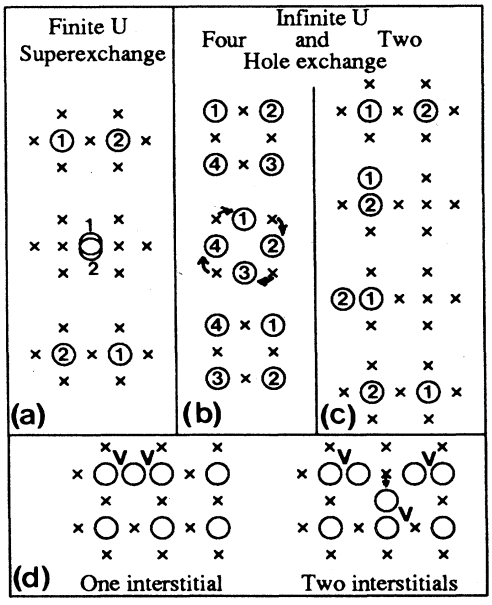

FIG. 1. (a) Pair exchange of two holes on Cu sites via double occupation of an intermediate O site (energy U). (b) Cyclic permutation of four holes on Cu sites via eight hops involving single occupation of O sites (double occupation forbidden by $U \to \infty$). (c) Pair exchange of two holes with $U \to \infty$. (d) Two isolated interstitial holes cost an energy $2(2V+\varepsilon)$, they can bind as shown on the right, with a shift of a neighboring Cu hole; the energy gain is $4V+2\varepsilon-(3V+3\varepsilon) = V-\varepsilon$.

(note that most current theories expected Heisenberg antiferromagnetism). These predictions for the 2D triangular solid are consistent with recent observations of 2D ferromagnetism in two ^{3}He solid layers adsorbed on grafoil.[8] This model also predicts ferromagnetism in the 2D Wigner solid near melting;[5] this remains to be tested experimentally.

We prove that with one hole per Cu site and in the large U_d limit Eq. (1) reduces to an effective spin-exchange model with dominant four-spin cyclic permutations. From exact diagonalization on small (up to 18 spins) clusters, we compare some physical properties of this model to that of a Heisenberg Hamiltonian. We show that there is an ordinary two-sublattice antiferromagnetic (AF) order at $T=0$ which does not correspond to the molecular-field (MF) expectation and presents more fluctuations than a Heisenberg model. We prove that the widths of the experimental two-magnon Raman spectra,[9] which are considerably larger than those expected for a Heisenberg Hamiltonian, are consistent with four-spin exchange. We determine the susceptibility $\chi(T)$ and find better agreement with experimental data compared to the predictions of a 2D Heisenberg model for both La_2CuO_4 and $YBa_2Cu_3O_6$ compounds. From the comparison of $\chi(T)$ for both models to experimental data for isostructural compounds, we argue that four-spin exchange could also occur in some Ni oxides.

By doping, additional holes are introduced on the O sites (the Cu^{3+} configuration is forbidden by the large U and O^- is more likely) and the system becomes a delocalized Fermi liquid. If the effective screened Coulomb repulsion between holes is short range, we prove that two interstitial holes could bind together, as shown in Fig. 1(d), to decrease the first-neighbor repulsion. Such a mechanism, as recently proposed for finite U_d,[3,10] could lead to a large effective attraction of order $V\sim 1$ to 2 eV, explaining high-T_c superconductivity.

To show the new correlations neglected in the simple Hubbard model with one hole per Cu site, we take $U_d/t\rightarrow\infty$ in Eq. (1) and use general perturbation in powers of t/V and $t/\varepsilon<1$ to derive an effective spin Hamiltonian. Since, in this limit, superexchange is suppressed, spin-exchange terms only appear at eighth order. Figure 1(b) shows eight successive hops via intermediate O sites on a square, leading to the cyclic exchange of four holes. Two-hole exchange can also occur at the same order through eight hops via neighboring O sites, as illustrated in Fig. 1(c). The effective exchange Hamiltonian is

$$\mathcal{H}_{ex}=-J\sum_{\substack{i,j\\ i<j}}P_{ij}-K_{SQ}\sum_{\substack{i,j,k\\ i<j<k<l}}(P_{ijkl}+P_{ijkl}^{-1}), \qquad (2)$$

with

$$J=\frac{-16t^8}{(\varepsilon+V)[(\varepsilon+V)(\varepsilon+2V)(2\varepsilon+V)]^2},$$

and

$$K_{SQ}=\frac{-4t^8}{(\varepsilon+V)^4(3\varepsilon+V)^2(2\varepsilon+V)^2}\times\left[\frac{(6\varepsilon+5V)^2}{\varepsilon}+\frac{(4\varepsilon+3V)^2(3\varepsilon+4V)^2}{(\varepsilon+2V)^2(\varepsilon+V)}\right].$$

P_{ij} and P_{ijkl} are two- and four-spin cyclic permutation operators corresponding to the permutations shown in Figs. 1(c) and 1(b). They can be expressed as functions of Pauli spin operators σ_i (see Refs. 4 and 6).

J is expected to be one order of magnitude smaller than K_{SQ}. For $\varepsilon\simeq 0.4$ eV, $V\simeq 1.5$ eV, $t\simeq 0.6$ eV, we obtain $|K_{SQ}|\simeq 0.045$ eV $\simeq 500$ K; $|J|\simeq 0.0006$ eV. For comparison, a superexchange process involving four hops and double occupancy of one O site with $U_0=10$ eV [Fig. 1(a)] ($U_{Cu}>U_0$) would lead to a pair exchange frequency $|J_{se}|\simeq 4t^4/U_0(\varepsilon+V)^2\simeq 0.014$ eV, three times smaller.

We now compare some properties of a pure four-spin exchange Hamiltonian [$J=0$ in (2)] with those of a Heisenberg model on a 2D square lattice. For both models, we express temperature, energies, and magnetic field in reduced units $T^*=T/-\Theta$, $E^*=-E/k_B\Theta$, $H^*=-\gamma\hbar H/2k_B\Theta$, with respect to the Curie-Weiss temperature $\Theta=3K_{SQ}$ or $\Theta=2J$, respectively.

With four-spin exchange only, the zero-field molecular-field (MF) state has four square sublattices with orthogonal magnetizations ($\uparrow,\rightarrow,\downarrow,\leftarrow$) [cf. Fig. 2(a)]. In a magnetic field $H_c^*\sim 0.43$, there is a first-order transition to a two-sublattice strongly canted phase ($\nwarrow,\nearrow$) [as in bcc ^{3}He (Ref. 6)] with a large magnetization $M=M_0(3H^*/8)^{1/3}$ saturating at $H^*=\frac{8}{3}$ to the maximum value M_0. However, at low field, the MF expectations can be incorrect in 2D. We have determined by the Lanczos method the exact zero-field ground state for

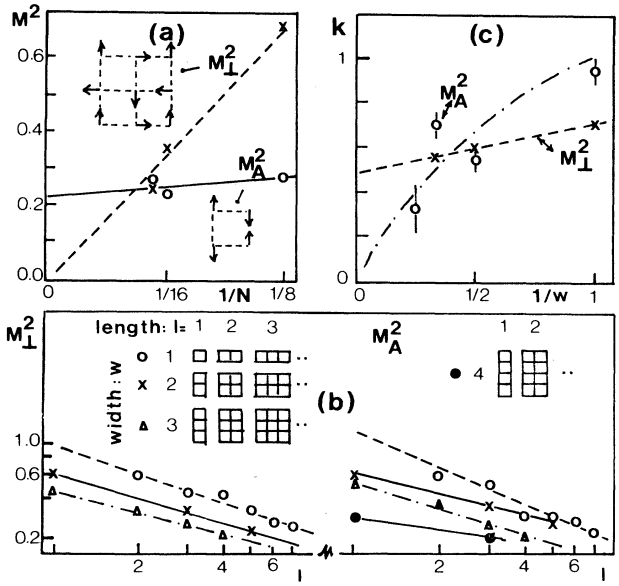

FIG. 2. (a) Staggered two-sublattice (M_A^2) and orthogonal four-sublattice ($M_\perp^2$) square magnetizations in terms of $1/N$ for square clusters with $N=8$, 16, 18 spins. (b) Logarithmic plots of $M_{A,\perp}^2$ for $w=1, 2, 3, \ldots$ rows of four-spin cycles in terms of the row length 1. For each w, an exponent k is deduced from the straight lines for $M_{A,\perp}^2\sim N^{-k}$; (c) k is plotted in terms of $1/w$. For $M_\perp$, k extrapolates to a finite value and there is no long-range order. For M_A, although less precise, the results indicate possible long-range order ($k\rightarrow 0$ as $w\rightarrow\infty$).

small systems of $N=4$ to 20 particles. For a general AF phase, with n sublattices A_λ, the order parameter is[11,12]

$$M_s=\left[3\left\langle\left[\sum_\lambda\sum_{j\in A_\lambda}\mathcal{R}_y^{-\alpha_\lambda}\sigma_j^z\mathcal{R}_y^{\alpha_\lambda}\right]^2\right\rangle\right]^{1/2}\Big/N,$$

where σ represents Pauli spin-$\frac{1}{2}$ matrices and $\mathcal{R}_y^{\alpha_\lambda}=\exp(-\frac{1}{2}i\alpha_\lambda\sigma_j^y)$ are rotation operators which, at each site, place the local z axis parallel to the MF spin direction. For ordinary AF order ($\uparrow,\downarrow$) with two alternate sublattices A_1, A_2, we obtain the usual staggered magnetization M_A with $\alpha_1=0$ and $\alpha_2=\pi$. For the four-sublattice phase ($\uparrow,\rightarrow,\downarrow,\leftarrow$), we take $\alpha_1=0$, $\alpha_2=\pi/2$, $\alpha_3=\pi$, $\alpha_4=3\pi/2$, and we call $M_\perp$ the corresponding order parameter. Two methods were used to obtain information about these correlations for $N\rightarrow\infty$. Figure 2(a) shows plots of M_A^2 and $M_\perp^2$, in terms of $1/N$, for $N=4$, 8, 16, 18 spin clusters with periodic boundary conditions as chosen in Ref. 13. The orthogonal magnetization $M_\perp$ corresponding to the MF state extrapolates to zero at $N\rightarrow\infty$, whereas the staggered magnetization tends to a finite value $M_A\sim0.45\pm0.05$. We also applied the method proposed in Ref. 12, replacing the "railroad-trestle" lattices by successive rows of four-spin cycles, with free boundaries. Figure 2(b) shows plots of M_A^2 and $M_\perp^2$ as a function of the lattice length for different widths (1,2,3,4,... ranges). For each width an exponent k is deduced for M_A^2 or $M_\perp^2\sim N^{-k}$. For both kinds of order, k is plotted in Fig. 2(c) in terms of the inverse width. For $M_\perp$, k extrapolates to a finite value for $N\rightarrow\infty$, proving definitely that $M_\perp$ is zero for the infinite system. Thus, the MF state is irrelevant, which is not surprising since (from the same methods) our estimation of the exact energy $E/N\simeq0.9K_{SQ}$ is far below the MF value $E_{MF}/N=0.5K_{SQ}$. The values of k for M_A are compatible with $k\rightarrow0$ for $N\rightarrow\infty$, leading to long-range order. In conclusion, we predict ordinary AF order at $T=0$ with a value $M_A\simeq0.45\pm0.05$, appreciably lower than that obtained with a Heisenberg Hamiltonian $M_A\simeq0.60$.[11] Taking $g\simeq2.2$ for Cu^{2+} in octahedral sites,[14] we expect an order parameter of $\simeq0.45g\mu_B/2\simeq0.5\mu_B$, in agreement with neutron diffraction.[1]

To obtain further information at finite temperature, we completely diagonalized both Heisenberg and four-spin Hamiltonians for square clusters of 8, 16, and 18 particles[13] with periodic boundary conditions.

A general result is that the density of states is broader for a four-spin exchange model, with a much larger number of low-lying excited states. This could explain the important inelasticity observed in both neutron scattering[15] and two-magnon Raman data.[9]

In Fig. 3, we compare for both Hamiltonians the squared matrix elements of the two-magnon Raman interaction at $T=0$ for a 16-spin cluster and yy geometry as defined in[9] $\mathbb{H}_R=C\sum_{i,j}(\hat{\mathbf{E}}_1\cdot\hat{\mathbf{r}}_{ij})(\hat{\mathbf{E}}_2\cdot\hat{\mathbf{r}}_{ij})\mathbf{S}_i\cdot\mathbf{S}_j$, the sum being performed on first neighbors.

Only one level contributes significantly to the spectrum for a Heisenberg Hamiltonian. It is centered around the peak predicted within the interacting spin-wave approximation[16] (dashed curve). This confirms the validity of spin waves for this model (note that recent Monte Carlo simulations[11] agree with the spin-wave prediction within a few percent for zero-point spin deviation); also the first $S=1$ excited states that we obtain in our diagonalization for a few values of k agree with the theoretical spin-wave spectrum: maximum E_M at $k=(\pi/a,0,0)$ and $E\simeq0.88E_M$ at $k=(\pi/2a,0,0)$ (we expect $E_M\sqrt{3}/2$ from spin waves).

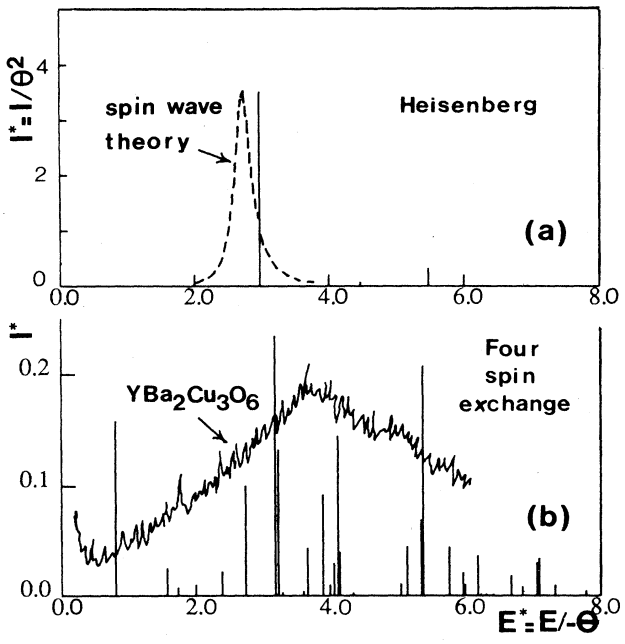

FIG. 3. Squared matrix elements $I=|\langle\phi_0|\mathbb{H}_R|\phi_E\rangle|^2$ of Raman interaction for 16-spin cluster, $|\phi_0\rangle$ and $|\phi_E\rangle$ represent, respectively, the ground state and excited state of energy E; the prefactor C in $\mathbb{H}_R$ has been taken to 1. Energy is normalized to $-\Theta$. (a) Heisenberg model: essentially one level is significant; it is close to the spectrum expected from spin-wave theory (Ref. 16) (dashed line). (b) The broad spectrum obtained with the four-spin model is compared to the experimental one in $YBa_2Cu_3O_6$ (Ref. 9) in yy geometry.

With a four-spin Hamiltonian, many levels contribute significantly to the Raman interaction and lead to a much broader spectrum [Fig. 3(b)]. The experimental spectrum observed at $T=20$ K in $YBa_2Cu_3O_6$ (Ref. 9) is compared. Its large width agrees quantitatively with the four-spin exchange predictions and is inconsistent with a Heisenberg model. Similar results which are not reported here are obtained by diagonalization of an 18-spin cluster. From the frequency corresponding to the maximum of the spectrum, which is close to that obtained with a Heisenberg model, we deduce a Curie-Weiss temperature $\Theta\simeq-1500$ K for both $YBa_2Cu_3O_6$ and La_2CuO_4; hence, $K_{SQ}\simeq-500$ K.

For both Hamiltonians, the inverse susceptibility $\chi^{-1}(T^*)$ for a 16-spin cluster (solid line) is plotted in Fig. 4. In the high-temperature range $T\geq|\Theta|$, these curves are compared to Padé approximations of high-temperature series expansions to 4th and 10th order for two- and four-spin exchange respectively (dashed lines). All plots are in reduced units $\chi^*=\chi/\chi_{CW}$,

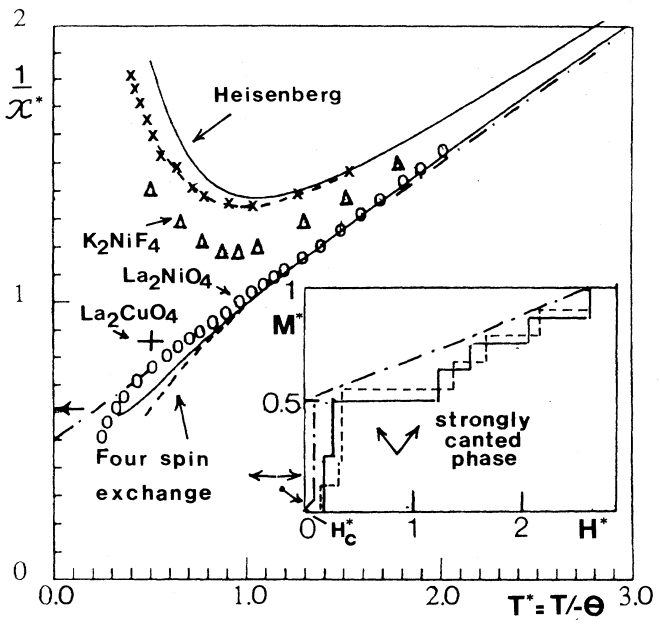

FIG. 4. Inverse susceptibilities for 2D Heisenberg and four-spin Hamiltonians. T is normalized to $-\Theta$ and χ to the Curie-Weiss value at $-\Theta$. Solid lines are from 16-spin cluster diagonalization and dashed lines are Padé approximants to high-temperature series expansion. The dash-dotted line is the Curie-Weiss law. The arrow shows the $T=0$ susceptibility, roughly extrapolated from calculations on 8, 16, 18-spin clusters. Experimental data are compared for 2D spin-$\frac{1}{2}$ $Cu(C_5H_5NO)_6(BF_4)_2$ (Ref. 20) (×) and spin-1 La_2NiO_4 (Ref. 19) (○) and K_2NiF_4 (Ref. 20) (△). The cross (+) represents the susceptibility of La_2CuO_4 around $\Theta/2\simeq 750$ K: $\chi\simeq 1.6\times 10^{-4}$ emu/mol is taken from Ref. 18, taking into account a diamagnetic contribution of -10^{-4} emu/mol. Inset shows the magnetization curves $M^*=M/M_0$ vs field H^* for $N=16$ spins (solid line) and $N=18$ (dashed line). The dash-dotted line represents the magnetization expected in the $N\sim\infty$ system, with a first-order transition to a strongly canted phase (↖,↗) at $H_c^*\sim 0.05$.

$\chi_{CW}=N(g\mu_B/2)^2/2k_B|\Theta|$ representing the Curie-Weiss value at $T^*=T/|\Theta|=1$. The Curie-Weiss law is represented by the dash-dotted line. As already observed in bcc ^{3}He, four-spin exchange enhances the susceptibility. The large deviation (−25%) from Curie-Weiss (CW) law at $T^*\sim 1$ observed in the 2D Heisenberg model is suppressed and $\chi^*(T^*)$ obeys Curie-Weiss law down to $\sim|\Theta|$. At lower temperatures χ^* further increases up to $\chi^*\simeq 1.5$ for $T^*=0.5$. In contrast, the 2D Heisenberg susceptibility presents a broad maximum just below $|\Theta|$ with $\chi^*\simeq 0.75$; its value at $T^*=0.5$ is $\chi^*\simeq 0.6$.

The Raman data give $\Theta\simeq -1500$ K within either a two- or four-spin exchange model. Taking this value, we expect at $T\simeq 750$ K a susceptibility of $\chi\simeq 1.5\chi_{CW}\simeq 2.2\times 10^{-4}$ emu/mol with four-spin exchange and $\chi\simeq 0.6\chi_{CW}\simeq 0.9\times 10^{-4}$ emu/mol with a Heisenberg Hamiltonian (we take $g=2.2$ for Cu^{2+} ion). For La_2CuO_4, taking into account the diamagnetic susceptibility of the ion core $\chi_{dia}\simeq -10^{-4}$ emu/mol,[17] one should expect a small negative experimental susceptibility, $\chi_{exp}\simeq -0.1\times 10^{-4}$ emu/mol, for a Heisenberg model and $\chi_{exp}\simeq 1.2\times 10^{-4}$ emu/mol with a four-spin exchange model; this latter value is in better agreement with experimental data[18] around 700 to 800 K. Similar values per Cu^{2+} mole can be deduced in $YBa_2Cu_3O_6$ and the same conclusion holds. Unfortunately, reliable experimental data are limited to a narrow temperature range around 500 to 800 K $\leq|\Theta|/2$ where both compounds are stable and where χ is not perturbed by 3D ordering or paramagnetic impurities.

We also compare, in Fig. 4, the experimental susceptibility for two AF compounds with lower $|\Theta|$ which are isostructural to La_2CuO_4. For La_2NiO_4 (Ref. 19) (circles) χ is strikingly close to the four-spin exchange predictions. Although spin-1 Ni^{2+} has two holes per site, we expect that small ε and strong on-site hole repulsion should still favor four-particle correlations. We have not calculated the χ curve for spin-1 and four-spin exchange but we expect the same behavior as observed with spin $\frac{1}{2}$ (the increase of χ with four-spin exchange is already seen in MF). In contrast K_2NiF_4 (Ref. 20) (triangles) exhibits the usual 2D Heisenberg behavior. From relation (2) our interpretation is straightforward: four-spin exchange dominates when ε is weak (in Cu-O, Ni-O, Ni-S). ε is much larger in halogenures like Ni-F, with stronger ionic bonding[2] and superexchange would then be predominant. Note that the exotic phase diagram of NiS_2, has been interpreted with four-spin exchange.[21]

The inset of Fig. 4 shows the magnetization for $N=16$ and 18 spins at $T=0$. A first-order transition to a state with large magnetization $M\sim 0.5M_0$ occurs at $H_c^*\sim 0.25$ proving that the MF strongly canted phase (↖,↗) is relevant at high field. This critical field decreases with N ($H_c^*\simeq 0.46$ for $N=8$), a rough linear extrapolation predicts H_c^* of order ~ 0.05 (within a factor of 2) for $N\to\infty$, corresponding to 100 T in La_2CuO_4 ($\Theta\simeq -1500$ K) and ~ 30 T in La_2NiO_4 ($\Theta\simeq -500$ K). Its experimental observation would be, as in bcc ^{3}He (Ref. 6) the best evidence of four-spin exchange interactions. This ferromagnetic tendency is characteristic of four-spin exchange. (The solution of the four-spin exchange Hamiltonian on a $N=4$ spin cluster gives two degenerate singlet and triplet ground states; the degeneracy is removed for $N>4$ but states with total spin $S\leq N/4$ remain relatively close to the singlet ground state.)

By doping La_2CuO_4 with Sr, or going from O_6 to O_7 in Y-Ba-Cu-O, additional holes are introduced on O sites in the 2D planes. With infinite U, in order to move, an interstitial has to push away a neighboring hole (like for two-particle exchange) and this reduces its mobility. Hence, we expect a Fermi-liquid behavior with T_F of the same order as exchange frequencies.[1]

An isolated interstitial increases the energy by $2V+\varepsilon$; if we consider a pair of interstitials they tend to bind together as shown in Fig. 1(d) with a repulsive shift of a neighboring Cu hole. Thus, the pair energy is $3V+3\varepsilon$ instead of $2(2V+\varepsilon)$. This strong attraction of order $V-\varepsilon$ can induce superconductivity. This type of process has been previously proposed for finite U_α,[3] it also exists in the infinite-U limit.[10] However, it is important to determine the limits for localization of such pairs as a function of t,

ε, and V. We emphasize that this attracting process disappears with second-neighbor Coulomb repulsion. It works if the Coulomb repulsion is screened, which is quite probable in these compounds with a high dielectric constant.

A similar pairing process between interstitials could eventually occur in Ni compounds. However, it would be of a different nature. In that case, in Fig. 1(d), two O holes are separated by a magnetic Ni^+ ion in $4d^9$ configuration (instead of a $4d^{10}$ nonmagnetic Cu^+). As a consequence of Hund's rule, the Ni^+ ion would polarize the surrounding O holes (only O holes with spin parallel to that of Ni^+ can move on Ni site) and singlet pairing would be suppressed.

For $U \rightarrow \infty$, the extended Hubbard Hamiltonian, Eq. (1), can lead to antiferromagnetism with unusual properties and superconductivity. In 2D, this model could apply as well for new superconductors and ^{3}He adsorbed on a substrate. Although 2D ^{3}He is usually triangular, some appropriate substrates could stabilize a square lattice and provide an interesting analogy to new superconductors with interplay of antiferromagnetism and superfluidity.

[1] *Proceedings of the International Conference on High-T_c Superconductors and Materials and Mechanisms of Superconductivity, Interlaken, Switzerland, 1988,* edited by J. Müller and J. L. Olsen [Physica C **153–155** (1988)].

[2] J. Zaanen, G. A. Sawatzky, and J. W. Allen, J. Magn. Magn. Mater. **54–57**, 607 (1986).

[3] J. E. Hirsch *et al.*, Phys. Rev. Lett. **60**, 1668 (1988).

[4] D. J. Thouless, Proc. Phys. Soc. London **86**, 905 (1965).

[5] J. M. Delrieu, M. Roger, and J. H. Hetherington, J. Low Temp. Phys. **40**, 71 (1980); J. M. Delrieu and N. Sullivan, Phys. Rev. B **23**, 3197 (1981); M. Roger, *ibid.* **30**, 6432 (1984).

[6] M. Roger, J. M. Delrieu, and J. H. Hetherington, Rev. Mod. Phys. **55**, 1 (1983).

[7] Y. Takano *et al.*, Phys. Rev. Lett. **55**, 1490 (1985).

[8] H. Godfrin, R. R. Ruel, and D. D. Osheroff, Phys. Rev. Lett. **60**, 305 (1988); M. Roger and J. M. Delrieu, Jpn. J. Appl. Phys. **26**, Suppl. 26-3, 267 (1987).

[9] K. B. Lyons *et al.*, Phys. Rev. Lett. **60**, 732 (1988).

[10] C. A. Balseiro *et al.*, Ref. 1, p. 1223.

[11] J. D. Reger and A. P. Young, Phys. Rev. B **37**, 5978 (1988).

[12] T. Oguchi, H. Nishimori, and Y. Taguchi, J. Phys. Soc. Jpn. **55**, 323 (1986).

[13] J. Oitmaa and D. D. Betts, Can. J. Phys. **56**, 897 (1978).

[14] J. W. Orton *et al.*, Proc. Phys. Soc. London **78**, 554 (1961).

[15] G. Shirane *et al.*, Phys. Rev. Lett. **59**, 1613 (1987).

[16] J. B. Parkinson, J. Phys. C **2**, 2012 (1969).

[17] F. Keffer, *Handbuch der Physik,* edited by S. Flugge (Springer-Verlag, Berlin, 1966).

[18] D. C. Johnston *et al.*, Phys. Rev. B **36**, 4007 (1987).

[19] G. A. Smolenski, V. N. Yudin, and E. Sher, Sov. Phys. Solid State **4**, 2452 (1963).

[20] L. J. De Jongh and A. R. Miedma, Adv. Phys. **23**, 1 (1974) (see p. 65); L. J. De Jongh, Solid State Commun. **65**, 963 (1988).

[21] K. Yoshida and S. Inagaki, J. Phys. Soc. Jpn. **50**, 3268 (1981).